

A reanalysis of EUV emission in clusters of galaxies

Stuart Bowyer¹, Thomas W. Berghöfer², and Eric Korpela¹

¹ Space Sciences Laboratory, University of California, Berkeley, CA 94720-7450, USA

² Max-Planck-Institut für extraterrestrische Physik, Giessenbachstraße, 85740 Garching, Germany

Abstract. We report a new analysis of diffuse EUV emission in clusters of galaxies. We find the cluster emission is strongly influenced by the variation of the telescope sensitivity over the field of view and upon the details of the subtraction of the EUV emission from the X-ray plasma. We investigate these effects on Abell 1795, Abell 2199, and the Coma cluster. When we use the appropriate correction factors, we find there is no evidence for any excess EUV emission in Abell 1795 or Abell 2199. However, we do find extended EUV emission in the Coma cluster and in the Virgo cluster using our new analysis procedures, confirming that in at least these clusters some as yet unidentified process is operative.

1. Introduction

Extreme ultraviolet (EUV) emission in excess of that produced by the well-studied X-ray emitting gas in clusters of galaxies has been reported in five clusters of galaxies. The effective bandpass of the EUVE telescope employed in these observations is defined by the intrinsic response of the telescope combined with the absorption of the intervening galactic interstellar medium (ISM). This bandpass has a peak at 80Å with 10% transmission at 66 and 100Å. A variety of instrumental effects that might have explained these results have been advanced but a detailed analysis has shown these factors cannot explain the data (Bowyer, Lieu & Mittaz, 1998).

It is interesting to note that the EUV excess is detected in some ROSAT images. However, the effect is sufficiently marginal that the ROSAT results can almost be explained away through the use of particular combinations of intervening Galactic ISM and its ionization state, and different cross sections for absorption by hydrogen and helium (Arabadjis & Bregman, 1999). The EUVE results, however, cannot be explained in this manner. It is also interesting to note that the EUV excess has been reported in every cluster investigated with EUVE.

A number of suggestions have been made as to the source of this EUV emission. Initial work focused on additional components of “warm gas” ($\sim 10^6$ K). The prob-

lem with this suggestion is that gas at this temperature is near the peak of the cooling curve and substantial energy is needed to supply the energy radiated away. One mechanism that can provide this energy is gravitational condensation. Cen & Ostriker (1999) have suggested that a pervasive warm intergalactic gas constitutes the majority of matter in the Universe; as this gas coalesces onto clusters of galaxies, it could produce the energy needed to sustain the EUV emitting gas.

Several authors (Hwang, 1997; Enßlin & Biermann, 1998) have suggested the EUV flux in the Coma Cluster is inverse Compton (hereafter: IC) emission produced by the population of electrons producing the radio emission scattering against the 3° K Black Body cosmic background. However, Bowyer & Berghöfer (1998) have shown that the existing population of radio emitting cosmic ray electrons cannot be responsible for the EUV emission in the Coma cluster, and some other population of cosmic rays will be required if this mechanism is the source of the EUV emission in this cluster. Lieu et al. (1999a) have suggested that the Coma cluster contains a large population of cosmic rays which are producing the 25 to 80 keV emission seen by BeppoSAX (Fusco-Femiano et al., 1999) and RXTE (Rephaeli, Gruber & Blanco 1999) via IC emission. They propose this population of cosmic rays extrapolated to lower energies will produce the observed EUV flux by IC emission. However, these authors have not addressed the fact that this population of electrons will produce a spatial distribution of the EUV flux which is inconsistent with the observational results of Bowyer & Berghöfer (1998).

Enßlin, Lieu, & Biermann (1999) have explored processes that might produce a heretofore undetected population of lower energy cosmic rays which could produce this flux. They demonstrate an evolutionary scenario in which relativistic electrons produced in the last merger event in Coma two Gyrs ago could produce these electrons. However, this model cannot produce the spatial profile of the EUV emission obtained by Bowyer & Berghöfer. They also consider IC scattering of starlight photons and show that under some scenarios this could account for the EUV flux and the required spatial distribution.

Sarazin & Lieu (1998) have suggested that all clusters of galaxies may contain a relic population of cosmic ray electrons that are unobservable in the radio and these will produce excess EUV flux by inverse Compton scattering against the 3° K cosmic background. Their proposal is based upon, and explains, details of the EUV data obtained on Abell 1795 (Mittaz, Lieu & Lockman, 1998).

We have obtained new data on some of these clusters and have analyzed archival data on others. We find that the results obtained are crucially dependent upon the characterization of the DS telescope, and upon details of the estimation of the EUV emission from the X-ray plasma. The results we obtain are quite different from those obtained in previous work.

2. Data and Data Analysis

All data were processed using procedures of the IRAF EUV package provided by the Center for EUV Astrophysics (CEA, Berkeley) which were especially designed for the analysis of EUVE data. As part of this process, we excluded detector events with pulse heights far from Gaussian peak of the photon pulse-height spectrum. Low energy events due to spurious detector noise ($\approx 15\%$ of the total), and high energy counts due to cosmic rays and charged particles ($\approx 25\%$ of the total), were screened out. A detailed description of different background contributions to the DS data can be found in Berghöfer et al. (1998). We point out that the location of the Gaussian peak in the pulse-height spectrum is not constant for all EUVE DS observations since the gain of the DS detector was changed periodically in the course of the mission. Consequently, pulse height limits were chosen individually for each DS observation. The resulting filtered event lists were corrected for electronic deadtime and telemetry throughput effects.

The background of the DS telescope consists of a uniform detector background, B_{int} , and a component that may vary over the field because of a variety of effects including vignetting, variations in the thickness of the filter covering the detector face, variations in the quantum efficiency over the face of the detector, and other causes. Hereafter we call this second component the vignetted background, B_{vig} . To investigate the possibility of a field variation effect, we chose four 20,000 s observations of blank sky with low and similar backgrounds that were obtained in a search for EUV emission from nearby pulsars (Korpela & Bowyer, 1998). We added 90,000 s of data from a blank field at R.A.₂₀₀₀ = $3^{\text{h}}31^{\text{m}}39^{\text{s}}$, Dec.₂₀₀₀ = $+18^\circ28'33''$ obtained from the EUV archives. *We emphasize that the images were added in detector coordinates, NOT sky map coordinates.* We processed the data as described above. We established that once proper pulse height selection of the detector events had been made, the detector backgrounds were all spatially identical.

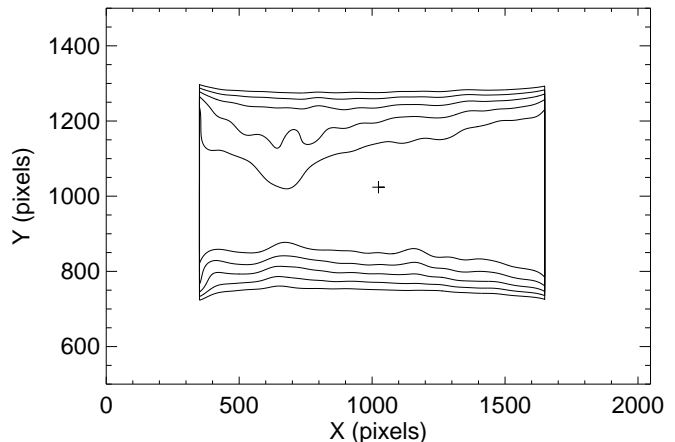


Fig. 1. A contour plot of counts obtained in long duration DS exposures showing the sensitivity variation of the DS Telescope over the field of view. We have cut the regions at the detector ends where the detector distortion becomes severe. The field displayed is approximately 1.75 degrees \times 0.73 degrees.

A contour plot of normalized count rates in these exposures convolved with a 32 pixel wide Gaussian is shown in Figure 1. The contours represent a 10% change in the measured count rates.¹ It is informative to compare this observationally derived result with the theoretically derived product provided in Sirk et al. (1997), which has been used in previous work on EUV emission in clusters and is essentially flat.

As a demonstration of the effect of this variation of telescope sensitivity in regards to studies of diffuse emission, we have derived azimuthally averaged radial intensity profiles of the EUV emission of the blank field shown in Figure 1 under the assumption that any background present was flat, following the procedures of Lieu et al. (1996) and Mittaz et al. (1998). One of these profiles was centered $15'$ to the left of the boresight, and one was centered $2'$ to the right of the boresight, following observation strategies often employed with EUVE. These results are shown as Figures 2a and 2b. These profiles clearly show (false) extended emission centered at these locations. A still different radial profile would be obtained at different locations on the detector and still different profiles would be obtained if data from any two locations were added.

In order to account for this telescope sensitivity variation in searching for true diffuse emission in clusters of galaxies, one must carry out detailed, though straightforward, processes.

All observations contain both B_{int} and B_{vig} . Because the ratio of these two backgrounds can vary, one must correct for this effect when scaling previously measured

¹ Investigators interested in using this observationally derived sensitivity plot may access Fits Files at "http://sag-www.ssl.berkeley.edu/~korpela/euve_eff".

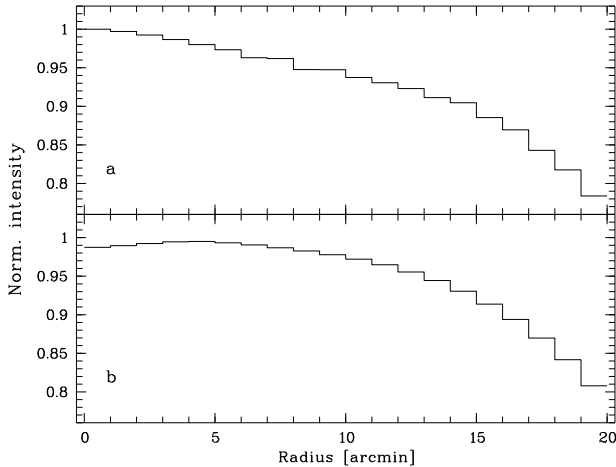


Fig. 2. a: The radial intensity profile of the EUV emission from the blank field shown in Fig. 1 with the assumption that any underlying background is flat. Fig. 2a shows the profile 15' to the left of the boresight and Fig. 2b shows the profile 2' to the right of the boresight. Both profiles show (false) diffuse emission; each is different because of differing telescope sensitivity variations at these locations.

backgrounds to the backgrounds of the new observations. The background subtracted image is:

$$I_{\text{net}} = I_{\text{on}} - B_{\text{int}} - fB_{\text{vig}} \quad (1)$$

where I_{on} is the on-source image. The term B_{int} is derived from measurements of the background in obscured regions of the detector covering about 3.5 % of the detector area. The term B_{vig} represents the vignettted background. The factor f is used to fit the vignettted background levels in the blank field with those of the on-source image. This factor is derived by fitting the observed photonic background with that of the blank field images in a region far from the source. Because of the long duration of the background exposures, the statistical errors in f are less than 1%. When comparing on-source and background in small detector regions, our errors are dominated by the count statistics of the region, rather than errors in the background fitting.

We have examined new data on Abell 1795 with the archival data on this cluster and find that the raw data from the new observations at $R > 2'$ (which excludes the effects of a bright transient source in the new data set) are identical within the counting errors, confirming the validity of the original data set used by Mittaz et al. (1998). Because the two data sets are identical and the more recent set is contaminated with a point source, we have used the archival data on Abell 1795 for our subsequent analysis.

We derived the azimuthally averaged radial intensity profile of the EUV emission of the cluster as a function of projected radius from the central core assuming spherical symmetry. The results are shown in Figure 3. Our

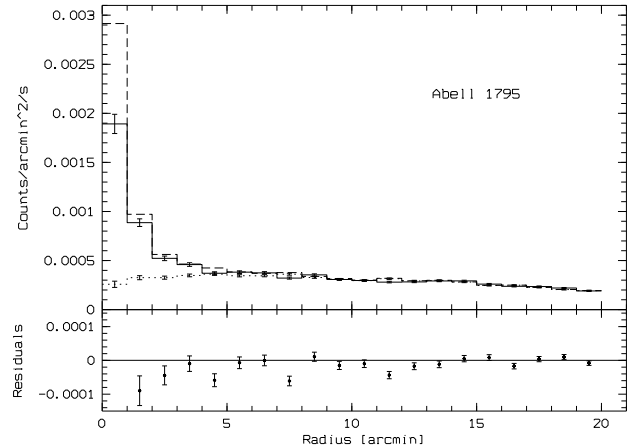


Fig. 3. The azimuthally averaged radial intensity profile of the EUV flux in Abell 1795 is shown as a solid line. The vignettted background from long observations of blank fields is shown as a dotted line. There is no excess EUV emission beyond 4'.

vignettted background, fitted at $R > 15'$, is shown as a dotted line. It is visually apparent that there is no excess EUV emission at radii larger than 4'. It is also clear that an improperly chosen background chosen at $R > 15'$ would result in apparent emission at smaller radii simply because of the effects of the vignettted background in the DS telescope.

We next determined the expected intensity and distribution of the EUV emission expected from the X-ray emitting plasma. We used the X-ray radial emission profile provided by Briel & Henry (1996). This profile was derived from ROSAT PSPC observations of the cluster in the energy band between 0.5–2.4 keV. At larger radii ($R > 4'$) this profile is well fit by a King profile (1972) with $\beta = 0.93$ and describes the large scale cluster X-ray emission with a temperature of 6.7 keV. The ROSAT observations also show a central excess emission within $R < 4'$. Briel & Henry (1996) obtained a temperature of 2.9 keV for this excess. We derived conversion factors for counts in the 0.5–2.4 keV band of the ROSAT PSPC to EUVE DS counts using these plasma temperatures. Our derivation employed the MEKAL plasma emission code with abundances of 0.3 solar. For a temperature of 6.7 keV we obtained a conversion factor of 126; the value for 2.9 keV was 110. We found that varying the temperature by ± 1 keV or using different abundances only affect these conversion factors by a few percent and thus changes of this nature would not significantly alter our results. We found that a deprojection of the emission components which takes into account the emission measures and sizes of the different components leads to the same result.

The correction for the intervening absorption of the ISM in our Galaxy will have a substantial impact on our results. Many workers simply apply the cross sections of Morrison & McCammon (1983) or Balucińska-Church &

McCammon (1992) for this correction, but there are several problems with this approach. The HeI absorption coefficient in this work is incorrect (Arabadjis & Bregman 1999). In addition, the ionization state of the ISM will substantially affect the result. The ISM absorption at EUV energies is primarily due to HI, HeI, and HeII; the metals in the list of Balucińska-Church & McCammon (1992) provide less than 30% of the absorption at wavelengths greater than 50 Å, and less than 10% at wavelengths greater than 100 Å, and none of the Galactic ISM is in the form of HeIII (see discussion below). Hence in general terms the absorbing material and related factors are given by:

$$N(\text{H}(\text{tot})) = N(\text{HI}) + N(\text{HII}) \quad (2)$$

$$N(\text{HeI}) = \frac{1}{10} [N(\text{H}(\text{tot}))] (1 - X(\text{HeII})) \quad (3)$$

$$N(\text{HeII}) = \frac{1}{10} [N(\text{H}(\text{tot}))] (X(\text{HeII})) \quad (4)$$

We have calculated the Galactic ISM absorption using these columns with HI cross sections of Rumph et al. (1994), HeI cross sections from Yan et al. (1998), and HeII cross sections from Rumph et al. We used these values with an improved estimate of the Galactic neutral hydrogen column density in the direction of Abell 1795 of $N(\text{HI}) = 0.95 \times 10^{20} \text{cm}^{-2}$ (J. Lockman, private communication). We assume the total helium is 10% of the total hydrogen column. A direct measurement of the HII column can be obtained, in principle, from measurements of the $\text{H}\alpha$ flux in this direction (Reynolds et al., 1998). Unfortunately, only an upper limit to this flux of $1 \times 10^{19} \text{cm}^{-2}$ is currently available (Haffner, private communication). A reasonable estimate for the HII column, based on all the available data, is that it is close to this upper limit (Reynolds, private communication). Consequently we have used this value for the HII column. The amount of HeII in this direction can be obtained from Fig. 1 of Bowyer et al. (1996). For A1795, $N(\text{H}(\text{tot})) = 1.1N(\text{HI})$, $N(\text{HeI}) = 0.1[1.1N(\text{HI})](1 - 0.02) = 0.108N(\text{HI})$, and $N(\text{HeII}) = 0.1(1.1N(\text{HI})) \times 0.02 = 2.2 \times 10^{-3}N(\text{HI})$. The absorption corrected results are shown in Figure 3 as a dashed line. The observed EUV emission is *less* than that produced by the X-ray plasma. This appears to be unphysical but is simply understood as discussed below.

After taking into account the vignetting and the EUV emission from the X-ray plasma, we see no excess EUV emission in this cluster.

We also examined archival data on Abell 2199 to ascertain whether a vignettted background could have produced an artificial extended diffuse EUV halo in this cluster. In Figure 4 we show the radial profile of the raw EUV data and the vignettted background fitted at $R > 15'$. It is apparent that there is no excess EUV emission beyond $8'$. We use the results of Siddiqui, Stewart, and Johnstone, (1998) to model the EUV emission from the X-ray gas in

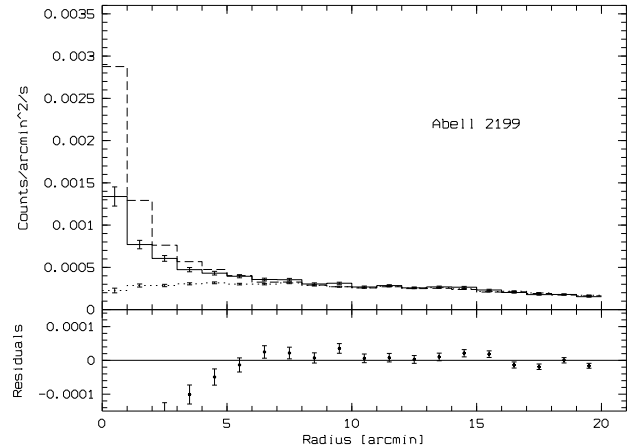


Fig. 4. The azimuthally averaged radial intensity profile of the EUV emission in Abell 2199 is shown as a solid line. The dotted line is the vignettted background. There is no EUV emission beyond $8'$.

the cluster. They found $T(\text{core}) = 2.9 \text{ keV}$ and $T(\text{outer}) = 4.08 \text{ keV}$. The conversion of the ROSAT X-ray profile into EUVE DS count rates has been done as described for Abell 1795. For Abell 2199 we found DS to PSPC hard band count rate ratios of 83.2 for $T = 2.9 \text{ keV}$ and 89.4 for $T = 4.08 \text{ keV}$. Absorption by the Galactic ISM was accounted for using $N(\text{HI}) = 8.3 \times 10^{19}$ (Lieu et al. 1999) with ionization fractions and cross sections as described previously. The results are shown in Figure 4 as a dashed line. Again, the expected EUV emission from the X-ray gas is larger than the observed flux, and there is no excess EUV emission in this cluster.

Finally, we re-examined the previously reported EUV excess in the Coma Cluster. We carried out our analysis using both of the existing DS images of this cluster. Because of the different roll orientation and pointing position in these images, it was necessary to carry out our analysis on each image individually. The results were then summed and the EUV emission and vignettted background are shown in Figure 5 as a solid and dotted line respectively. In this figure, we have fit the vignettted background to the Coma observations beyond $17'$; however, because faint emission due to the cluster likely extends past this point, especially in the direction of the NGC 4874 sub-cluster, this is likely to be a slight overestimate of the background and hence the excess EUV emission we derive may be a slight underestimate. If the X-ray profile of the Coma Cluster is used as a guide, we expect this effect to be small compared to the statistical errors in each radial bin.

The X-ray profile has been constructed using ROSAT PSPC archival data of Coma. We verified that our PSPC hard band cluster profile is consistent with the profile provided by Briel, Henry & Böhringer (1992) but includes the central excess associated with the galaxy group around NGC 4874. We assumed that this X-ray emission is due

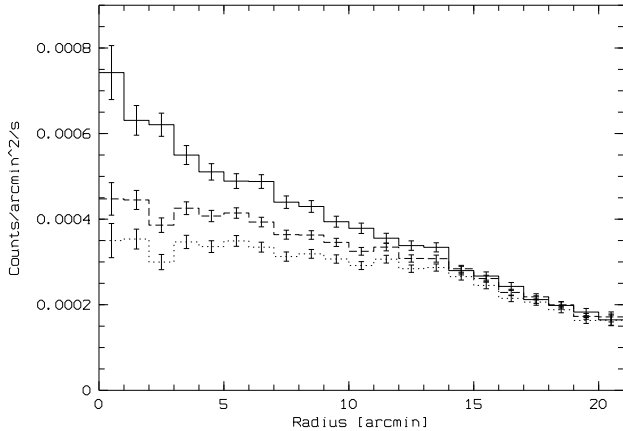


Fig. 5. The azimuthally averaged radial intensity profile of the EUV flux in the Coma cluster is shown as a solid line. The expected EUV emission from the X-ray plasma is shown as a dashed line. The vignettted background is shown as a dotted line.

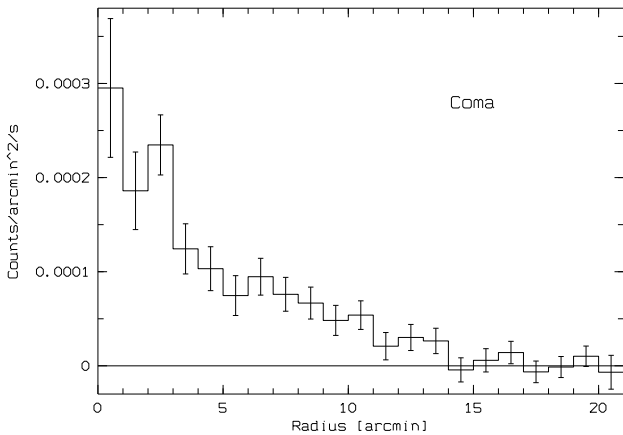


Fig. 6. The excess EUV emission in the Coma cluster.

to a plasma at $T = 9$ keV (Donnelly et al., 1999) absorbed by a hydrogen column of $8.7 \times 10^{19} \text{cm}^{-2}$ (Lieu et al., 1996) with ionization fractions and cross sections for Galactic absorption as described above. Here we obtained a DS to PSPC hard band conversion factor of 112.

The residual EUV emission in excess of the expected contribution of the X-ray gas shown in Figure 6 demonstrates that there is, indeed, excess EUV emission in the Coma cluster.

Based on our new analysis technique we also confirm excess EUV emission in the Virgo cluster of galaxies. Details are provided in Berghöfer & Bowyer (this workshop). In Figure 7 we provide a plot of the excess EUV emission in the central part of the Virgo cluster. Clearly, there is EUV emission in excess of the expected low energy tail of the X-ray emitting gas in Virgo.

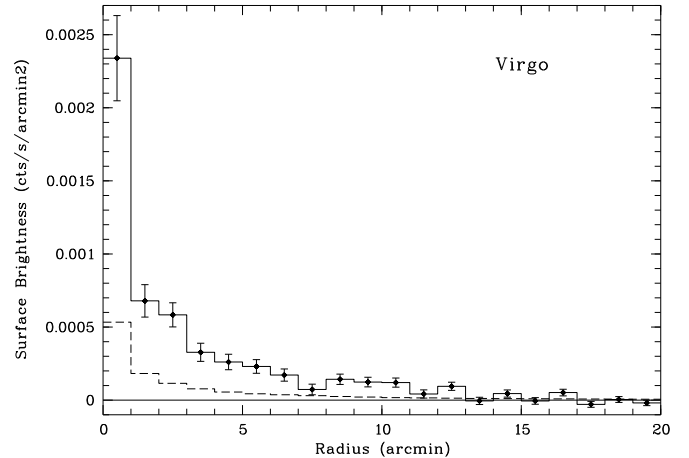


Fig. 7. The excess EUV emission in the center of the Virgo cluster (solid line) in comparison to the expected contribution of the X-ray emitting cluster gas (dashed line).

3. Discussion

The results of our new analysis show no excess EUV emission at radii larger than $4'$ for Abell 1795 and $8'$ for Abell 2199 contrary to previous work on these clusters. When we consider the inner regions for these clusters, we find the results expected are dependent upon a proper evaluation of the EUV emission from the X-ray plasma. When this emission is properly accounted for, the expected EUV emission from the X-ray plasma is *less* than is actually produced. This can be understood in terms of excess absorption within the cluster core. This effect has been noted in studies of X-ray cluster emission in cooling flows, where it is often reported that the hydrogen column density is larger in the core of the cluster. There is no observational evidence for more hydrogen in these regions, and neutral hydrogen is not expected in this environment. A reasonable explanation for this effect is that the X-ray reduction codes employed in these analyses require more absorption for a reasonable fit, and this is achieved blindly by adding more hydrogen with a standard admixture of non-ionized metals. It is more likely that in the cooler regions of the cooling flow, some metals are not completely ionized and these ions produce the extra absorption of the X-ray flux (Allen et al. 1996). This absorption would be even more substantial for the EUV flux, and would produce the effects seen. We point out that a study of the differing amount of absorption in the EUV and X-ray bands may provide sufficient information to identify the primary absorbing species.

When we employ our new analysis techniques with the data on the Coma cluster we find there *is* excess EUV emission confirming the results of previous studies. However, the distribution of this flux differs in detail from that previously reported. The distribution of this radiation is shown in Figure 6, along with the count rate intensity. The

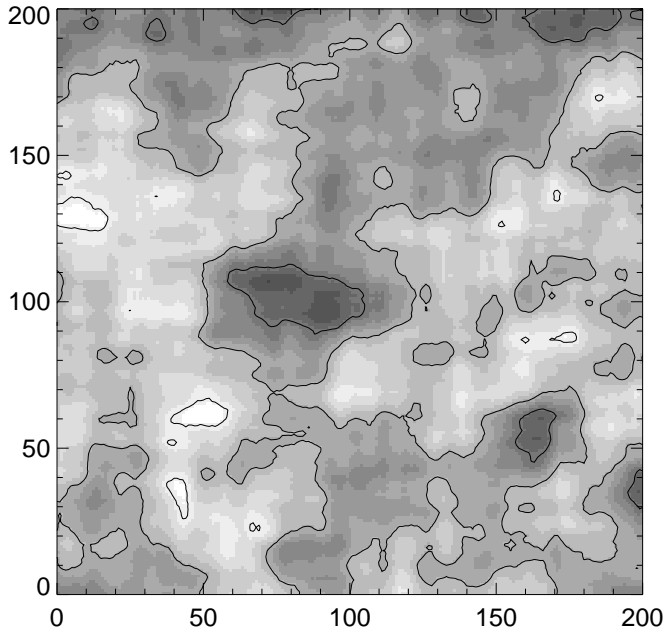


Fig. 8. Variations in the blank field image for a 15' field of view centered upon the detector coordinates where the EUVE observation of A 2199 was made. The background was smoothed to 2'. Gaussian count statistics give expected uncertainties of 2.6%. The contours are 90%, 100%, and 110% of the mean and are each separated by 3.8σ .

intensity in physical units is (slightly) dependent upon the assumed spectral distribution of the flux. A source with a photon spectral index of 1.6 results in an EUV source luminosity of $1.5 \pm 0.5 \times 10^{42} \text{ergs}^{-1}$.

It is useful to consider why our results are different from those of Mittaz et al. (1998), and Lieu, Bonamente & Mittaz (1999). While it is difficult to evaluate the details of another researchers' analysis, it is clear that a key difference is our use of an observationally derived vignettted background. Mittaz et al. and Lieu et al. used the theoretical background function (Richard Lieu, private communication) which is essentially flat. In addition, these authors also carried out their analysis of the EUV flux without first removing the non-photon background from their data. The extent to which this affects the results is not substantial, as we obtain the same general picture with data that has not been processed in this manner. Their approach to estimating the EUV emission produced by the X-ray plasma is also different than ours.

It is interesting to ask why both the analyses of Lieu et al and that presented here do show excess diffuse EUV emission in the Coma cluster and the Virgo cluster. The primary explanation is that both of these clusters do, in fact, have excess EUV emission. This emission is sufficiently extended that the effects of the vignettted background, though changing the details of the results, do not dominate as they do in Abell 1795 and Abell 2199.

Finally, we have examined the effects of fine grained detector variations on the data obtained from any point in the sky. As one example in Fig. 8 we show variations in the blank field image for a 15' field of view centered upon the detector coordinates where the EUVE observation of A 2199 was made. The image has been smoothed to 2'. Count statistics give expected uncertainties of 2.6%. The contours are 90%, 100% and 110% of the mean and are separated by 3.8σ . A wavelet analysis of this data as presented by Richard Lieu (this conference) would obviously show substantial effects, which would be entirely due to this fine scale structure in the detector. This structure varies over the face of the detector. Consequently the image taken at different locations will be different, which will tend to confuse uncareful workers.

4. Conclusions

We investigated the effects of the telescope sensitivity variation over the field of view and found this was a key factor in investigating extended EUV emission in clusters of galaxies. Our study shows why excess EUV emission has been found in every cluster examined to date with EUVE. *Any* point in the sky will show extended EUV emission using the analysis employed in previous studies of clusters of galaxies. We also used a detailed approach to the evaluation of the EUV flux produced by the X-ray gas in the core regions of these clusters.

We find no evidence for excess EUV emission in Abell 1795 or Abell 2199. We do, however, confirm extended EUV emission in the Coma cluster and Virgo cluster although the distributions of these fluxes are different in detail from that previously reported. The fact that we do find extended EUV emission in the Coma cluster and Virgo cluster using our new analysis procedures confirms that an unidentified processes is operative in this cluster.

Acknowledgements. We acknowledge useful discussions with Michael Lampton, Pat Henry, John Vallergera, Carl Heiles, Richard Lieu, John Mittaz and Jean Dupuis. This work was supported in part by NASA contract NAS 5-30180. TWB was supported in part by a Feodor-Lynen Fellowship of the Alexander-von-Humboldt-Stiftung.

References

- Allen, S., Fabian, A., Edge, A., Bautz, M., Furuzawa, A., & Tawara, Y. 1996, MNRAS, 283, 263
- Arabadjis, J. S. & Bregman J. N., 1999, ApJ, 514, 607
- Balucińska-Church, M. & McCammon, D. 1992, ApJ, 400, 699
- Berghöfer, T. W., Bowyer, S., Lieu, R. & Knude, J. 1998, ApJ, 500, 838
- Bowyer S., Lampton M. & Lieu, R. 1996, *Science*, 274, 1338
- Bowyer S., Lieu, R. & Mittaz, J. P. 1997, IAU Symposium No. 153: The Hot Universe, eds. K. Koyama et al., Dordrecht: Kluwer, 185
- Bowyer, S. & Berghöfer, T. W. 1998, ApJ, 506, 502

- Briel, U. G., Henry, J. P. & Böhringer, H. 1992, *A&A*, 259L, 31
- Briel, U. & Henry, J. P. 1996, *ApJ*, 472, 131
- Cen, R. & Ostriker, J. 1999, *ApJ*, in press
- Donnelly, R. H., Markevitch, M., Forman, W., Jones, C., Churazov, E. & Gilfanov, M. 1999, *ApJ*, in press
- Enßlin, T. & Biermann, P. 1998, *A&A*, 330, 96
- Enßlin, T., Lieu, R. & Biermann, P. 1999, *A&A*, 344, 409
- Fusco-Femiano, R., Dal Fiume, D., Feretti, L., et al. 1999, *ApJ*, 513, L21
- Hwang, C.-Y. 1997, *Science*, 278, 1917
- King, I. 1972, *ApJ*, 174, L123
- Korpela, E. & Bowyer S. 1998, *ApJ*, 115, 2551
- Lieu, R., Mittaz, J., Bowyer, S., et al. 1996, *Science*, 274, 1335
- Lieu, R., Ip, W.-H., Axford, W. & Bonamente, M. 1999, *ApJl*, 510, L25
- Lieu, R., Bonamente, M. & Mittaz, J. 1999, *ApJ*, in press
- Mittaz, J., Lieu, R. & Lockman, F. 1998, *ApJl*, 498, L17
- Morrison, R. & McCammon, D. 1983, *ApJ*, 270, 119
- Rephaeli, Y., Gruber, D. & Blanco, P. 1999, *ApJ*, 511, 21
- Reynolds, R. J., Tufte, S. L., Haffner, L. M., Jaehnig, K., & Percival, J. W. 1998, *Pub. Astron. Soc. Aus.*, 15, 14
- Rumph, T., Bowyer, S. & Vennes, S. 1994, *AJ*, 107, 2108
- Sarazin, C. & Lieu, R. 1998, *ApJ*, 494, L177
- Siddiqui, H., Stewart, G. & Johnstone, R. 1998, *A&A*, 334, 71
- Sirk, M. M., Vallerga, J. V., Finley, D. S., et al. 1997, *ApJS*, 110, 347
- Yan, M., Sadeghpour, H. & Dalgarno, A. 1998, *ApJ*, 496, 1044